Chapter 14

Electric Breakdown Model for Super-Thin Polyester Foil

Haiyang Wang and Zhengzhong Zeng

Additional information is available at the end of the chapter

http://dx.doi.org/10.5772/48478

1. Introduction

Polyester has been more and more widely applied to the field of electrical insulation because of their excellent electrical and mechanical properties. One of the commonest concerns in industry is the reliability of materials. Therefore, the study of breakdown of solid dielectrics is extremely important in industrial applications. The increasing demanding for polyester films requires that the dielectric strength of polyester with various film thicknesses should be measured accurately. Lack of accurate data on dielectric strength could lead to design shortcomings: excessive insulation could lead to more expensive equipments, while inadequate insulation could lead to premature failure. The data of breakdown strength for polyester from several hundred microns to several millimeters can be directly obtained from the handbook of dielectric materials. However, there are few data of breakdown strength in micro-meter regime.

The dielectric strength of solid dielectrics is affected by many factors, such as ambient temperature, humidity, duration of test, impurities or structural defects, whether a.c., d.c. or impulse voltages are being used, pressure applied to these electrodes etc. The mechanism of breakdown is complex in the case of solids, and varies depending on the time of application of voltage as shown Fig. 1 (Naidu & Kamaraju, 1995; Pai & Zhang, 1995). The various mechanisms are intrinsic breakdown (Callen, 1949; Hippel & Alger, 1949; O'Dwyer, 1964; Seeger & Teller, 1939; Seitz, 1948; Whitehead, 1951), electromechanical breakdown (Laghari & Sarjeant, 1992; Stark & Garton, 1955), breakdown due to treeing and tracking, thermal breakdown, electrochemical breakdown (Sawa, 1986).

1. Intrinsic Breakdown -- it is generally considered to be due to electrons in the insulator gain sufficient energy from the applied field to cross the forbidden energy gap from valence to the conduction band. Intrinsic breakdown is usually accomplished in the order of 10^{-8}s (Seeger & Teller, 1939).

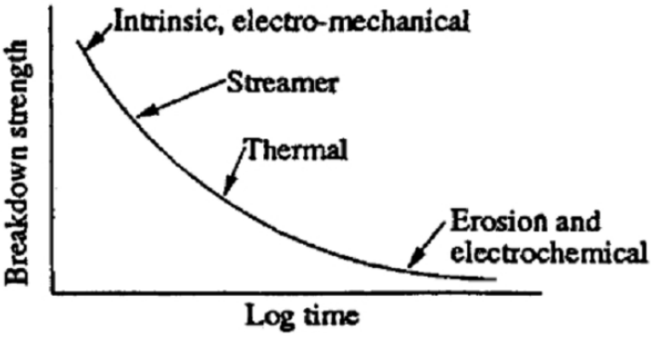

Figure 1. Variation of breakdown strength with time after application of voltage

2. Streamer Breakdown -- the mechanism is conceptually similar to the streamer mechanism in gases, namely when the avalanche exceeds certain critical size breakdown will occur. Transit time is usually short.
3. Thermal breakdown -- when an insulator is stressed electrically, because of currents and dielectric losses due to polarization, heart is continuously generated within the insulator. If the rate of heat generation exceeds the rate of heat losses, then the insulator will undergo thermal breakdown. Such breakdown takes place usually in a much slower time scale.
4. Erosion Breakdown -- insulators of contain voids or cavities within the material. These cavities are usually filled with gas or liquid medium of lower breakdown strength than the solid insulator. Accordingly, under normal working stress of the insulator the voltage across the cavities may exceed the breakdown value hence initiating breakdown in the cavities.
5. Breakdown due to tracking and other causes -- Tracking is the formation of some permanent conducting paths, usually carbon, along the insulator surface due to degradation of the insulator or other causes.
6. Electromechanical breakdown – Electromechanical breakdown occurs in dielectric foils of low Young's modulus and easy deforming and it is because of the force of attraction between the surface charges.
7. Treeing breakdown -- treeing occurs due to the erosion of material at the tips of the spark. Erosion results in the roughening of the surfaces, and hence becomes a source of dirt and contamination. This causes increased conductivity resulting either in the formation of conducting path bridging the electrodes or in a mechanical failure of the dielectric.

Electrical breakdown testing of polymers for insulator applications has long been a subject of interest. In order to improve insulator performance, it is essential to understand the mechanisms of electrical breakdown in solid dielectrics. However, unlike the case for gases, electrical breakdown and conduction mechanisms in polymeric solids are less understood. In solid dielectrics, the electrical transport phenomena include currents due to orientation and interfacial polarization in addition to electronic and ionic charge carriers (Barber et al., 2009). On account of the time of dielectric breakdown, this chapter mainly presents intrinsic breakdown and electromechanical breakdown.

2. Intrinsic breakdown

When an electric field is applied to an insulator, electrons gain sufficient energy from the applied field to cross the forbidden energy gap from the valence band to conduction band. When this process is repeated, more and more electrons become available in the conduction band, eventually leading to breakdown. Intrinsic breakdown usually occurs in the order of 10-8s. The initial density of free electrons is assumed to be large, and electron-electron collisions occur. The critical criterion of intrinsic breakdown is initial electrons formed by impact ionization. It consists of Hippel's low-energy criterion and Frohlich's high-energy criterion (Callen, 1949; Frohlich, 1939; Hippel & Alger, 1949; O'Dwyer, 1964; Seeger & Teller, 1939; Seitz, 1948; Whitehead, 1951).

2.1. Hippel low-energy criterion

Hippel low-energy criterion assumed that the energy E breakdown occurs when the applied field is high enough to accelerate electrons of any given energy in the conduction band to sufficient energy to further ionize the ions of the crystal by collision, thus leading to an exponential increase in the number of electrons in the conduction band. It may be easily seen that the applied field necessary to accelerate (on the average) an electron of given energy has a maximum when considered as a function of electron energy. In order to accelerate an electron, the applied field must compensate the energy lost by this electron to the lattice; but slow electrons have insufficient energy to excite the vibrational modes of the lattice, whereas very fast electrons interact for too short a time with the ions which they pass to transfer energy to them with appreciable probability. The breakdown strength, according to von Hippel's "low energy" criterion, therefore corresponds to the maximum, and an electron brought into the conduction band with low energy is immediately accelerated to the ionization energy and produces an additional conduction electron, the process thus building up in the form of an avalanche.

2.2. Frohlich high-energy criterion

Frohlich high-energy criterion is based on that an applied field sufficient only to accelerate electrons already having the ionization energy may lead to an instability and to electric breakdown (Callen, 1949; Cooper, 1966).

Eq. (1) shows the critical breakdown strength of intrinsic electron breakdown (Callen, 1949). For low energy breakdown theory $u = u_c \approx 4\hbar\omega$, and for high-energy breakdown theory, $u = u_I$.

$$E_{\mathrm{B}} = \sqrt{\frac{m^* B}{e^2 \tau}} \tag{1}$$

Eq. (1) may be written as

$$E_{\mathrm{B}} = E_0 \sqrt{\frac{\hbar\omega}{C} \cdot \frac{1}{\tau} \cdot \frac{B}{C}} \tag{2}$$

Where

$$E_0 = \frac{\sqrt{2}\pi m^* e e^{*2}}{Ma^3 \hbar\omega} \tag{3}$$

B is the average rate of energy loss for a given electronic energy, and is expressed by Eq. (4), where u is the average effect of collisions on the electrons of energy. C is expressed by Eq. (5). τ is the relaxation time, e is charge of electron, e^* is the effective charge per ion, m^* is the effective mass of the electron, M is the reduced mass of the ions, a is the interionic distance, ω is the natural angular frequency and ω_t is the natural angular frequency of the transverse mode.

$$B(u) = C\left(\frac{\hbar\omega}{u}\right)^{1/2}\left[(\overline{n}+1)\ln\frac{1+(1-\hbar\omega/u)^{1/2}}{1-(1-\hbar\omega/u)^{1/2}} - \overline{n}\ln\frac{1+(1+\hbar\omega/u)^{1/2}}{1-(1+\hbar\omega/u)^{1/2}}\right] \tag{4}$$

$$C = \frac{\pi(2m^*)^{1/2}e^2}{Ma^3(\hbar\omega)^{1/2}} \tag{5}$$

$\overline{n}$ is the average probability of scattering of an electron and is given by

$$\overline{n} = \frac{1}{e^{\hbar\omega/kT}-1} \tag{6}$$

Where k is Boltamann's constant =8.622×10^{-5} eV/°C.

$$\omega^2 = \frac{2\pi e^{*2}}{Ma^3}\left(\frac{\varepsilon_r\varepsilon_{op}}{\varepsilon_{op}-\varepsilon_r}\right) \tag{7}$$

$$\frac{\omega^2}{\omega_t^2} = \frac{\varepsilon_r}{\varepsilon_{op}} \tag{8}$$

$$\frac{1}{\tau} = \frac{B}{2\hbar\omega}\sqrt{\frac{\hbar\omega}{u}} + \frac{C}{\hbar\omega}\sqrt{\frac{\hbar\omega}{u}}\left[(\overline{n}+1)\sqrt{1-\frac{\hbar\omega}{u}} + \overline{n}\sqrt{1+\frac{\hbar\omega}{u}}\right] \tag{9}$$

Where e^* is expressed in terms of ω by Eq. (7) and ω is expressed in terms of ω_t by Eq. (8). We obtain

$$E_0 = \frac{2^{3/2}\pi^2 m^* e}{\hbar^2}\hbar\omega_t\frac{\varepsilon_r-\varepsilon_{op}}{(\varepsilon_r\varepsilon_{op}^3)^{1/2}} = 1.34\times10^8(\hbar\omega_t)\frac{\varepsilon_r-\varepsilon_{op}}{(\varepsilon_r\varepsilon_{op}^3)^{1/2}} \tag{10}$$

$$E_{BH} = \frac{E_0}{C}\sqrt{\frac{\hbar\omega B(T,u)}{\tau}} \quad \left(u = u_c \approx 4\hbar\omega\right) \tag{11}$$

$$E_{\mathrm{BF}} = \frac{E_0}{C}\sqrt{\frac{\hbar\omega B(T,u)}{\tau}} \quad \left(u = u_{\mathrm{I}}\right) \tag{12}$$

Where ε_{r} and $\varepsilon_{\mathrm{op}}$ are the relative and optical values of the dielectric constant, T is the temperature of the lattice in K.

Material	ε_{r}	$\varepsilon_{\mathrm{op}}$	a/ 10^{-10}m	M/ 10^{-20}g	E_{BH} / (kV•mm^{-1})	E_{BF} / (kV•mm^{-1})	E_{E} / (kV•mm^{-1})
PE	2.4	2.28	2.52	2.8	79	17	20
polycarbonate	3	2.5	20.8	40	255	54	90
polyester	3.2	10.7	3	301	65	65	180

Table 1. Breakdown strength for polymer

In Table 1 the pertinent breakdown strength data for polymer are shown according to Eq. (10) and Eq. (11). The electron energy is 0.1～0.2 eV for Hippel's criterion and 5 eV for Frohlich's criterion. The theoretical values are compared with the experimental breakdown strengths in mm regime. The experimental breakdown strength E_{E} which is given by Ref. (Wang et al. 1992) in mm regime is less than the breakdown strength of Hippel's criterion E_{BH} and greater than the breakdown strength of Forhlich's criterion E_{BF}. The critical breakdown strength of intrinsic breakdown model is calculated on the basis of Hippel's low-energy criterion and Frohlich's high-energy criterion (Wang et al., 2008).

3. Electromechanical breakdown

3.1. Electromechanical breakdown

Electromechanical breakdown is likely to happen in dielectric foils of low Young's modulus and easy deforming. When a dielectric foil is subjected to a high voltage, an electrostatic compressive force which will cause deformation of the dielectric foil is produced. If the electric stress exceeds the mechanical compressive strength of the dielectric foil, breakdown of the dielectric foil takes place. The electromechanical breakdown model is shown in Fig. 2. If the thickness of the specimen is d_0 and is compressed to d under an applied voltage U, then the electrically developed compressive stress is in equilibrium

$$\varepsilon_0\varepsilon_{\mathrm{r}}\frac{U^2}{2d^2} = Y\ln\left(\frac{d_0}{d}\right) \tag{13}$$

Where Y is the Young's modulus.

A plot of thickness as a function of voltage on normalized scales is given in Fig. 3. It is obviously seen that there is a critical voltage above which the thickness goes to zero. This occurs when $d[d(U)]/dU = -\infty$ or $d(U)/d[d(U)] = 0$. Therefore, the critical breakdown strength of electromechanical breakdown is (Laghari & Sarjeant, 1992; Stark & Garton, 1955)

$$E_{\mathrm{EM}} = \frac{U}{d_0} = 0.6\left(\frac{Y}{\varepsilon_0 \varepsilon_{\mathrm{r}}}\right)^{1/2} \tag{14}$$

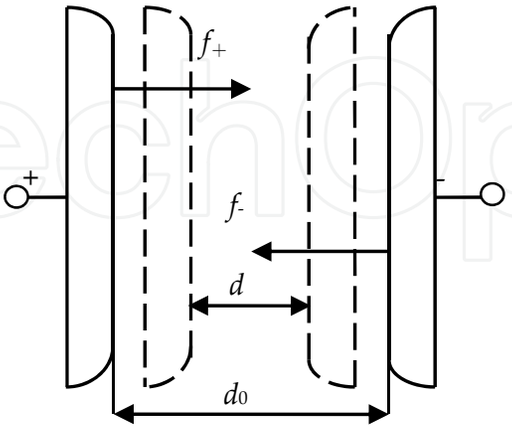

Figure 2. Electromechanical breakdown model

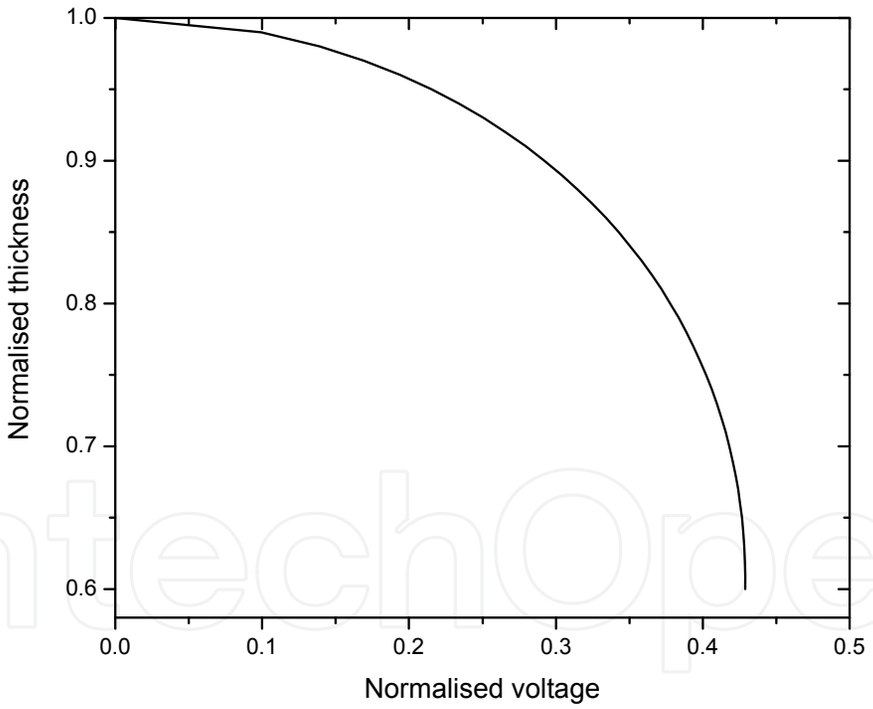

Figure 3. Thickness as function of voltage for electromechanical breakdown

The electromechanical breakdown model is rather unrealistic as it assumed that the dielectric material somehow disappeared to an infinitesimal thickness at $U \geq U_{em}$. Therefore, it may ignore several factors, such as possible earlier instability at microscopic areas of stress concentration, the dependence of Y on time and stress and plastic flow. Stack and Garton pointed out that the stress concentration at microscopic areas is instable, which may result in a localized thinning and breakdown. Blok and LeGrand considered that local

regions subjected to higher-than-average electric fields and experienced a shear stress which tended to form an indentation. The indentation gives rise to an even more inhomogeneous field, produces a sharp depression and eventually causes the material to flow radially away (Blok & LeGrand, 1969).

3.2. Electrofracture breakdown

Zeller et al (Zeller et al., 1984; Zeller & Schneider, 1984) proposed electrofracture as an aging mechanism in which the growth of a filamentary crack through a dielectric was caused by electrostatic forces. The model is based on the concepts of fracture mechanics in which the change in electrostatic energy at growth is equal to the mechanical energy required for partial discharge channel formation.

In the electrofracture mechanism the local field at the crack tip is considered to be insufficiently high for the strain energy density W_{em} contribution to be insignificant, i.e. electrostatic energy density $W_{es} \gg W_{em}$. So that the criterion for electrofracture is:

$$W_{es} \gg W_p \tag{15}$$

The electrofracture breakdown strength at the end of the crack tip is given by

$$E_{\mathrm{EF}} = \left[\frac{2\Upsilon}{\varepsilon_0 \varepsilon_r} \right]^{1/2} \tag{16}$$

E_{EF} is the local field at the tip of the crack whereas the electromechanical breakdown field is the applied field.

3.3. Filamentary electromechanical breakdown

Fothergill proposed the filamentary electromechanical breakdown in which a filamentary-shaped crack propagates through a dielectric releasing both electrostatic energy and electromechanical strain energy stored in the material due to the applied electric field (Fothergill, 1991, 1992). It operates at higher local fields.

The filamentary electromechanical breakdown model assumed electric field at the filament tip that are sufficiently high for $W_{em} > W_{es}$, so that the appropriate criterion is:

$$W_{em} > W_s + W_p \tag{17}$$

The filamentary electromechanical breakdown strength is defined as

$$E_{\mathrm{FEM}} = \left(\frac{8\Upsilon(2G + \Upsilon r_f)}{\varepsilon_0^2 \varepsilon_r^2 r_f} \right)^{1/4} \tag{18}$$

In general, $2G \gg \Upsilon r_f$, so that eq. (18) is written as (Hikita et al., 1987)

$$E_{\mathrm{FEM}} = \left(\frac{16GY}{\varepsilon_0^2 \varepsilon_r^2 r_f} \right)^{1/4} \tag{19}$$

A modified relationship between applied voltage and electric field at the tip of a filament is given by Eichhorn (Eichhorn, 1977) as:

$$E = \frac{V(1 + r_f / d)^{1/2}}{r_f \ \arctan h((1 + r_f / d)^{-1/2})} \tag{20}$$

Where d is the distance from the filament to the counter electrode, and is assumed to be the full thickness of the specimen in the worst-case estimate. r_f is the tubular crack of radius and depends on what initiates the filament. If it is assumed of $E = U / r_f$, the radius of the filament can be predicted from eq. (20). Solving eq. (20) give $r_f = 0.29 \mu m$ which is quite reasonable.

Both the electrofracture and filamentary electromechanical breakdown mechanisms assume a crack propagation process. The limiting speed of a crack is equal to that of a longitudinal elastic wave in the material.

According to the Young's modulus of different materials and Eq. (14), Eq. (16) and Eq. (19), the critical strengths of polyester, polyimide, polycarbonate, PE and polypropylene are obtained. The results are shown in Table 2, from which it is apparent that the critical strength of electric-mechanical breakdown is higher than the strength given by Ref. (Wang et al. 1992) in the mm regime. Therefore, the above results support the electric-mechanical breakdown mechanism for relatively thinner dielectric foils.

Material	Y/ (MN•m^{-2})	G/ (J•m^{-2})	ε_r	E_{EM} / (kV•mm^{-1})	E_{EF} / (kV•mm^{-1})	E_{FEM} / (kV•mm^{-1})
polyester	35	3600	3.2	667	1554	633
polyimide	28	6000	3.5	571	1330	542
polycarbonate	30	3000	9.2	638	1486	606
PE	9.2	3800	2.3	410	955	389
polypropylene	16	7900	2.2	544	1267	516

Table 2. Critical strength of materials

4. Recent development in polymer breakdown theory

Many studies have been published on high-field electrical conduction and breakdown of insulating polymers and there are also many good reviews and books which deal with this subject (Bartnikas & Eichhorn, 1983; Ieda, 1980, 1984; O'Dwyer, 1973). However, the dielectric breakdown processes of polymers are complicated due to their highly complex structures. Therefore, much work has been devoted to clarify the correlation between the breakdown characteristics and the properties inherent to polymers. Theories on the breakdown mechanisms are usually divided into three categories: electronic, thermal (Hap & Raju, 2006) and mechanical processes.

The different degrees of ordering of macromolecules and the presence of regions of varying densities gives rise to different conductivities under an applied field. A non-uniform voltage drop occurs within the polymer when a current begins to flow, leading to variable distribution of electric field. A detailed analysis of breakdown processes in polymers has been discussed by Ieda et al (Ieda, 1980). Artbauer proposed the basic idea of Free Volume Theory (Artbauer, 1996), which was taken in explaining the breakdown phenomena of polymer around the glass transition temperature. The amorphous phase in polymers with unoccupied volume consisting of holes of molecular order presents a free path for the electrons to accelerate under an external field and gain energy. Job et al. improved dielectric strength of polymers by chemical modifications. They have increased the breakdown strength of polyethylene terephthalate (PET) films by *insitu* polymerization of a layer of polyaniline (PANI). A 30% increase in dielectric strength was observed when the non-conductive PANI filled the voids of PET. And they proposed the breakdown was the electron avalanche process (Job et al., 2003). Breakdown in polymers with saturated bonds, such as polyethylene and polypropylene, can not be explained by the electron avalanche mechanism as they have a short free path length. As a result, the electrons cannot gain sufficient energy by acceleration to cause avalanche. In these polymers, electrical breakdown is the last step in a process of polymer degradation that results in the formation of conducting channels. The formation of these conducting channels depends on the intensity and time of the applied external field. The lifetime of these polymers decreases exponentially with applied electric field (Zakrevski et al., 2003). Overall, a general consensus has emerged that the reduction in dielectric breakdown strength of polymers is closely related to the dissociation (bond scission) of polymer molecules under an applied external field. The dissociation process is considered to be the initiation of polymeric breakdown. However, the exact mechanism of dissociation is unclear. One approach to explain this phenomenon is the non-uniform distribution of electric field intensity within a polymer due to electrode defects and inherent differences within the structure of polymer (Zakrevski et al., 2003).

The dielectric breakdown field of polyimide (PI) thin films has been studied across the temperature range from 25 to 400 °C under dc conditions by Diaham et al. it appeared that both the breakdown field value and β–scale parameters decrease with increasing electrode area following the area extrapolation law. It was found that the β–parameter has presented an unexpected increase with increasing the thickness thanks to percolation theories (Diaham et al., 2010).

Peruani et al described the dielectric breakdown model in conductor-loaded composites. Conducting particles are distributed at random in the insulating matrix, and the dielectric breakdown propagates according to new rules to take into account electrical properties and particle size. Dielectric breakdown patterns are characterized by their fractal dimension and the parameters of the Weibull distribution. Studies are carried out as a function of the fraction of conducting in homogeneities. The fractal dimension of electrical trees approaches the fractal dimension of a percolation cluster when the fraction of conducting particles approximates the percolation limit (Peruani et al., 2003). DammigQuiña et al developed a capacitive dielectric breakdown model (CDBM) of electrical tree growth to simulate dielectric breakdown in polymer materials. Dependence of the fractal dimension on the applied voltage, the breakdown process has its thermodynamic origin in the interplay

between energy injection and space charge formation processes. The model is capable of predicting electrical trees with fractal dimensions and qualitatively reproducing the temporal evolution of the breakdown process (DammigQuiña et al., 2008).

Kim and Shi investigated the dielectric strength of an interlevel low relative permittivity dielectric for various film thicknesses and temperatures by using I-V measurements with metal-insulator-semiconductor (MIS) structures. It is found that the dielectric breakdown mechanism is electromechanical in origin for relatively thick films (thickness >500 nm). The dielectric strength is proportional to the square root of Young's modulus of the films (Kim & Shi, 2001).

5. Experimental

5.1. Polyester foil

The polyester foil studied here is compound of biaxially-oriented polyethylene terephthalate, as shown in Fig. 4. Biaxially-oriented Polyethylene terephthalate, commonly abbreviated BOPET, is made from stretched polyethylene terephthalate (PET) and used for its high tensile strength, chemical and dimensional stability, transparency, gas and aroma barrier properties and electrical insulation (Sarker et al., 2001).

The end properties of the BOPET are direct consequence of their super molecular structure. The final structure of the BOPET depends mainly by the melt spinning conditions and by the subsequent heat-mechanical modifications, too. The desirable super molecular structure and the needed final morphologies and properties of the PET can be obtained by controlling of the forming process parameters as well as the subsequent treatment. For example, BOPET can be metallized by vapor deposition of a thin film of evaporated aluminum, gold, or other metal onto it. Metallized BOPET film, along with other plastic films, is used as a dielectric in foil capacitor. Four film thicknesses of 9μm, 12μm, 15μm and 18 μm were selected to study the breakdown strength.

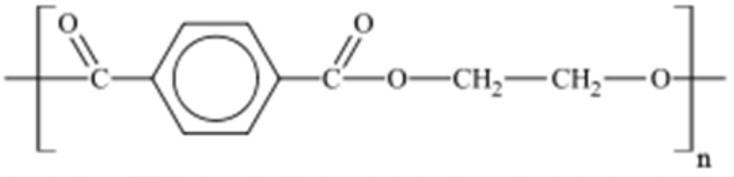

Figure 4. Chemical structure of the Polyethylene terephthalate

5.2. Experimental setup

Dielectric breakdown field measurements have been performed using a dc voltage supplied by a 15 kV voltage source connected to the sample. The electrical schematic diagram is shown in Fig. 5. In Fig. 5, 1, 2 and 6 are transmission lines. 3 is the polymer-foil switch. 4, 5 are the charging resistance. The breakdown field was identified when the polymer-foil switch is self-breakdown, and output a rectangular pulse. The maximum voltage supplied was also recorded using a divider connected to the generator and was considered as the breakdown voltage (Wang et al., 2004, 2006).

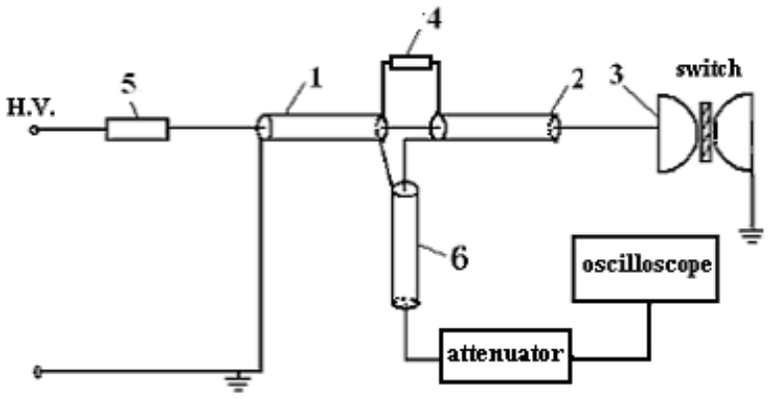

1,2,6 transmission line; 3 polymer-foil switch; 4,5 charging resistance

Figure 5. Electrical schematic diagram of experiment

Fig. 6 is the experimental arrangement of polyester-foil switch. The high voltage electrode (HE) and ground electrode (GE) are planes made of copper, and between HE and GE is the polyester foil, whose thickness varies among 9μm, 12μm, 5μm and 18μm. The self-breakdown voltage is attained by a resistive divider. The measurement is accomplished by a 500MHz digital storage oscilloscope.

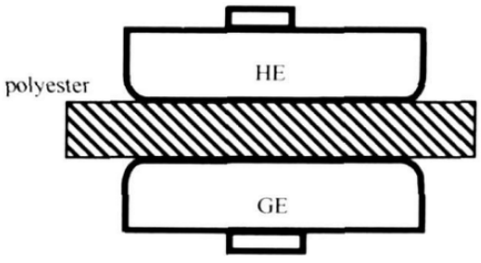

Figure 6. Experimental setup

6. Statistical analysis

Although a number of samples of the same material may be tested, each sample might exhibit breakdown at a different voltage due to random structural and measurement differences. The breakdown voltage can be considered as a random variable, which necessitates a statistical analysis of the breakdown data. Electrical breakdown can be considered as a system failure under the condition where a weak link in the system fails. The Weibull distribution, which is a type of extreme value distribution, is the most common for such applications (Weibull, 1951; Wu & Vollertsen, 2002).

$$F(x) = 1 - e^{-(\frac{x-\gamma}{\alpha})^{\beta}} \tag{21}$$

Where $F(x)$ is the cumulative probability of failure, α is the scale parameter (V/cm) corresponding to a probability of failure $F(\alpha)$ =63.2%, β is the shape parameter. A high β-value is related to a low scattering of the data. The location (or threshold) parameter γ has been set to zero.

The experimental data have been ranking using the median rank approximation given by (Chauvet & Laurent, 1993; Fothergill, 1990):

$$F(i,n) = \frac{i - 0.3}{n + 0.4} \tag{22}$$

Where, i and n are the rank of a failed sample and the total number of tested samples, respectively. For plotting the Weibull distribution law, the transformation of equ. (21) into equ. (23) has been realized:

$$\log_{10}\left[\log_e\left(\frac{1}{1-F(x)}\right)\right] = \beta\left[\log_{10}(x) - \log_{10}(\alpha)\right] \tag{23}$$

The Weibull parameters have been extracted considering a confidence interval of 90 %. Both the maximum likelihood and least square fit methods have been also applied leading to similar α– and β–parameter values (Diaham et al., 2010; Laihonen et al., 2007a, 2007b).

7. Results and discussion

Experiments were performed to measure the self-breakdown voltage of 10μm level foil. Fig. 7 and Fig. 8 show self-breakdown voltage and deviation thickness-varied polyester foils under positive voltage, respectively. The dashed lines through the data points represent the average self-breakdown voltage of the foils. From Fig. 7, it is clearly seen that the average self-breakdown voltage under positive voltage for 9μm, 12μm, 15μm, 18μm foils are 4.2, 5.7, 7.2 and 9.3 kV respectively, and the corresponding standard deviations are 0.6, 0.5, 0.8 and 0.9 kV. As shown in Fig. 8, the breakdown strength for 9, 12, 15, 18μm foils under positive voltage are 467, 475, 480 and 517kV/mm, and the corresponding standard deviations are 67, 42, 51 and 50 kV/mm, respectively.

Compared to the dielectric strength of thickness in mm regime, it can obviously that the breakdown strength for 10μm level foil is far greater than that breakdown strength in mm regime. That is named 'film strengthenization effect'. Nevertheless, as far as the breakdown strength for those four kinds of thickness foils are concerned, it exhibits a slight increase with increasing thickness for our results. It seems to be contrary to the film strengthenization effect. The reasons for this phenomenon are surface roughness conditions of electrodes, thickness deviation, defects and treatment processing, and so on. This 'curious' behavior also can be interpreted with the percolation theory. It based on a priori supposed that when the probability to find defects into the bulk increases, an increase in the scattering of the breakdown and a decrease in the shape parameter value ought to be observed (Diaham et al., 2010; Essam, 1980; Helgee&Bjellheim, 1991).

Fig. 9 and Fig. 10 show self-breakdown voltage and breakdown strength for thickness-varied polyester foils under negative voltage, respectively. The average self-breakdown voltage under negative voltage for 9, 12, 15, 18μm foils are 3.8, 5.4, 7.4, and 9.0kV respectively, and the corresponding standard deviations are 0.5, 0.7, 0.4 and 0.9 kV. The

breakdown strength for 9, 12, 15, 18μm foils are 444, 450, 490 and 500kV/mm, and the corresponding standard deviations are 53, 58, 28 and 49 kV/mm. It is also found that the breakdown voltage and dielectric strength of polyester film under negative voltage is smaller than that one under positive voltage. In other words, the dielectric strength of polyester film is evidently dependent of the voltage polarity. It can be interpreted by the space charge effect in relation to polyester solid structure (Ieda, 1987).

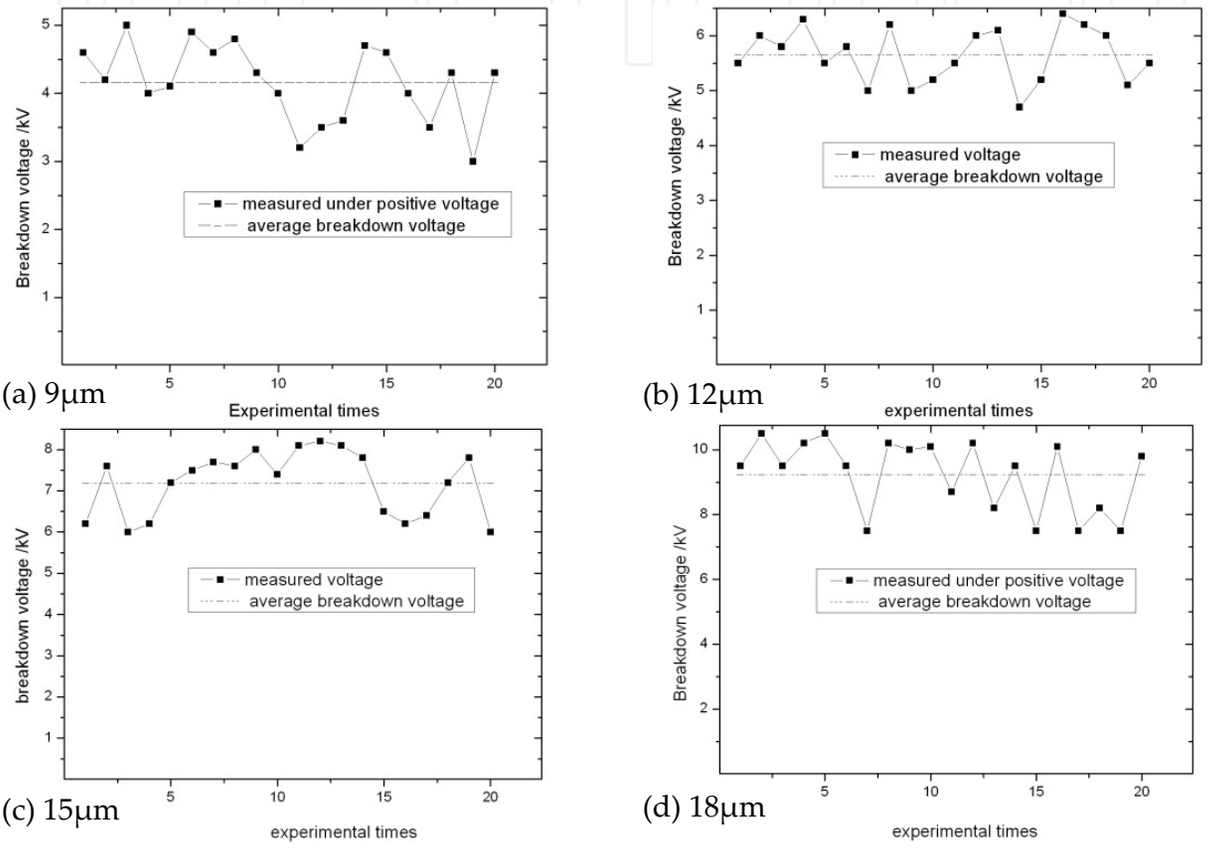

Figure 7. Self-breakdown voltage of thickness-varied polyester-foils under positive voltage

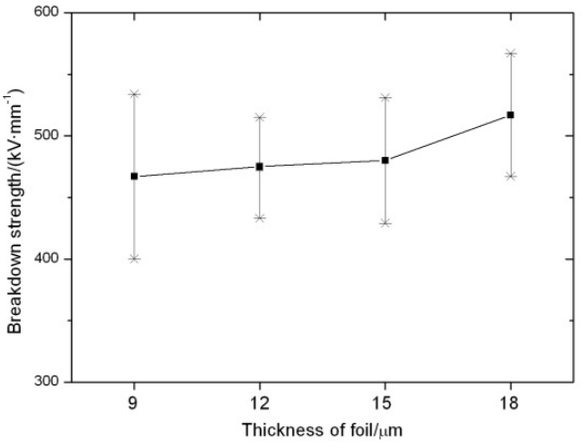

Figure 8. Breakdown strength for thickness-varied polyester-foil under positive voltage

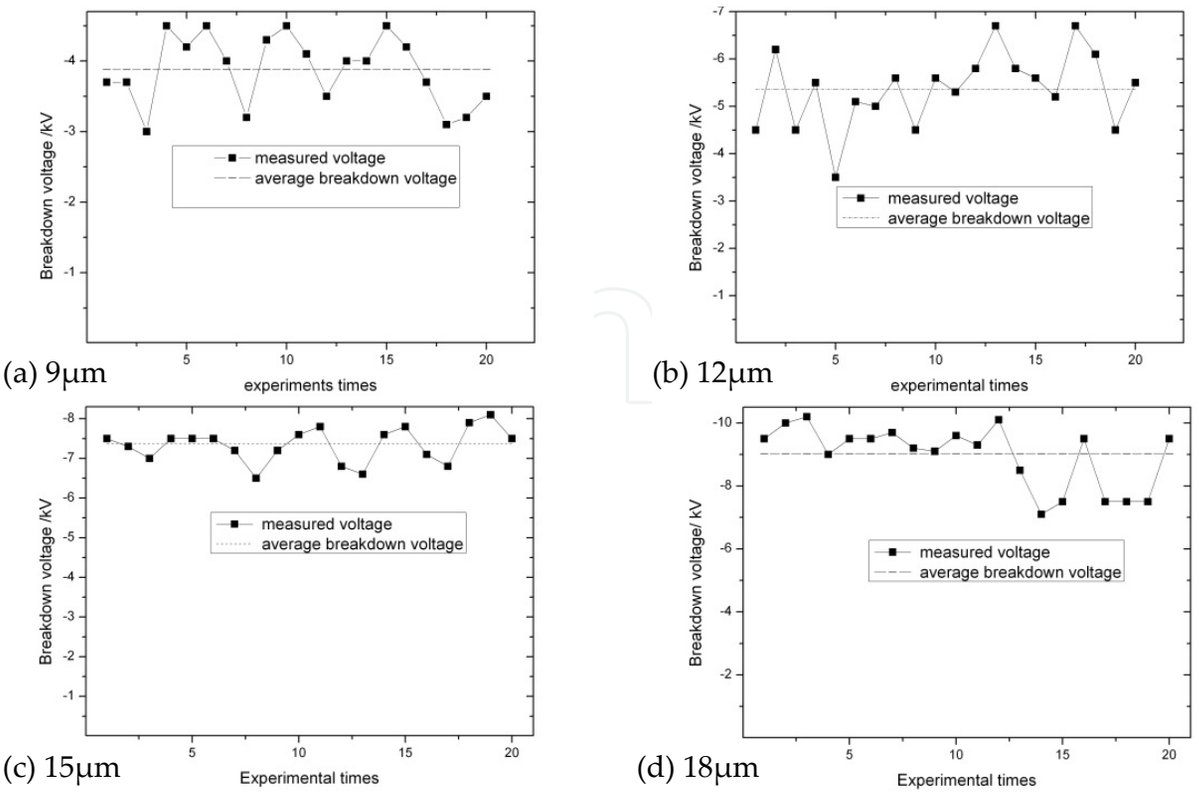

Figure 9. Self-breakdown voltage of thickness-varied polyester-foils under negative voltage

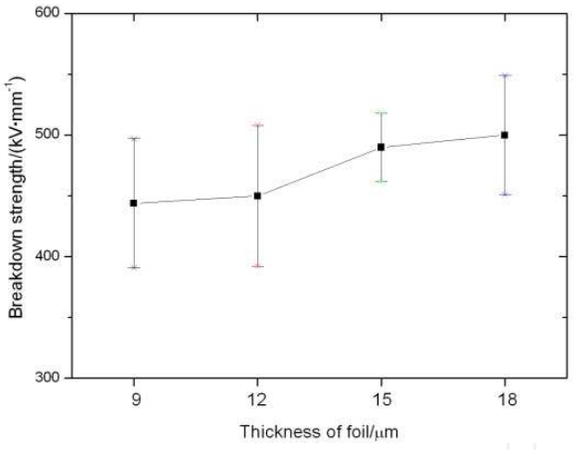

Figure 10. Breakdown strength for thickness-varied polyester-foil under negative voltage

The influence of the thickness on the Weibull parameters was also investigated. Fig. 11 shows the α–parameter values in a plot versus the polyester film thickness. The solid line and dash line represent the linear fits. This result is not in good agreement with typical value found in the literature for polymers and for such a litter variation of the thickness (Diaham et al., 2010; Helgee&Bjellheim, 1991).

In comparison with the theoretical results, the experimental results show that the critical breakdown strength of the polyester film in the intrinsic breakdown model is far lower than

the experimental results and the critical breakdown strength of the polyester film in the electromechanical breakdown model and filamentary electromechanical breakdown model almost agrees with the experimental data of the polyester film. Therefore, it is concluded that the dielectric breakdown mechanism for thickness in micro-meter range is dominantly controlled by the electromechanical breakdown mechanism.

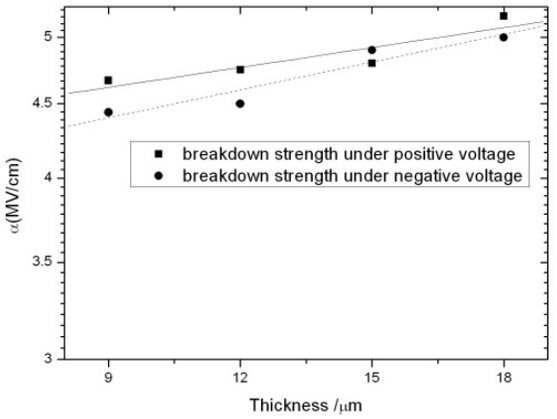

Figure 11. Changes in the scale parameter versus the polyester-foil thickness

8. Conclusion

The theoretical and experimental results of dielectric strength of polyester films in micro-meter regime are presented. Theoretical analysis was carried out based on the intrinsic breakdown model and the electromechanical breakdown model. The critical breakdown strength of intrinsic breakdown model is estimated on the basis of Hippel's low-energy criterion and Frohlich's high-energy criterion. The electromechanical breakdown model, electrofracture and filamentary electromechanical breakdown model are also introduced. The thickness dependence of dielectric strength of the polyester films was also investigated in a plane-plane electrode arrangement with different polar DC voltage. The thickness of the polyester films varied among 9μm, 12μm, 15μm and 18μm. Experimental results show that there is greatly increasing on the dielectric strength in micro-meter regime, compared to the dielectric strength of thickness in mm regime. Nevertheless, it exhibits a slight decrease with increasing thickness for our results. This 'curious' behavior is discussed on the basis of the percolation theory. It is also found that the dielectric strength of polyester film under negative voltage is smaller than that one under positive voltage. In other words, the dielectric strength of polyester film is evidently dependent of the voltage polarity. It can be interpreted by the space charge effect in relation to polyester solid structure. The comparison between the theoretical analysis and the experimental results is also presented. The results show that the critical breakdown strength of the polyester film in the intrinsic breakdown model is far lower than the experimental results, and the critical breakdown strength of the polyester film in the electromechanical breakdown model almost agrees with the experimental data of the polyester film. Therefore, it is concluded that the dielectric breakdown mechanism for thickness in micro-meter range is dominantly controlled by the electromechanical breakdown mechanism.

Author details

Haiyang Wang and Zhengzhong Zeng
Northwest Institute of Nuclear Technology, Xi'an, People's Republic of China

9. References

Artbauer, J. (1996). Electric Strength of Polymers. *J. Phys. D: Appl. Phys.,* Vol. 29, No. 2, (February 1996), pp. 446-457, ISSN 0022-3727.

Barber, P.; Balasubramanian, S.; Anguchamy, Y.; Gong, S. S.; Wibowo, A.; Gao, H. S.; Ploehn, H. J. & Zur Loye, H. -C. (2009). Polymer Composite and Nanocomposite Dielectric Materials for Pulse Power Energy Storage. *Materials,* Vol. 2, No. 4, pp. 1697-1733, (October 2009), ISSN 1996-1944.

Bartnikas, R. & Eichhorn, R. M. (1983). *Engineering Dielectrics. Volume IIA—Electrical Properties of Solid Insulating Materials: Molecular Structure and Electrical Behavior,* ASTM Publication, ISSN 978-0-8031-0228-6, Baltimore.

Blok, J. & LeGrand, D. G. (1969). Dielectric Breakdown of Polymer Films. *J. Appl. Phys.,* Vol. 40, No. 1, (January 1969), pp. 288-293, ISSN 0021-8979.

Callen, H. B. (1949). Electric Breakdown in Ionic Crystals. *Phys. Rev.,* Vol. 76, No. 9, (November 1949), pp. 1394-1402, ISSN 0031-899X.

Chauvet, C., & Laurent, C. (1993). Weibull Statistics in Short term Dielectric Breakdown of Thin Polyethylene Films. *IEEE Trans. Electr. Insul.,* Vol. 28, No. 1, (February 1993), pp. 18-29, ISSN 0018-9367.

Cooper, R. (1966). The Electric Strength of Solid Dielectrics. *Br. J. Appl. Phys.,* Vol. 17, No. 2, (February 1966), pp. 149-161, ISSN 0508-3443.

DammigQuiña, P. L.; Herrera, L.; Irurzun, I. M. & Mola, E. E. (2008). A Capacitive Model for Dielectric Breakdown in Polymer Materials. *Computational Materials Science,* Vol. 44, No. 2, (December 2008), pp. 330-338, ISSN 0927-0256.

Diaham, S.; Zelmat, S.; Locatelli, M. L.; Dinculescu, S.; Decup, M. & Lebey, T. (2010). Dielectric Breakdown of Polyimide Films: Area, Thickness and Temperature Dependence. *IEEE Trans. Dielectr. Electr. Insul.,* Vol. 17, No. 1, (February 2010), pp. 18-27, ISSN 1070-9878.

Eichhorn, R. M. (1977). Treeing in Solid Extruded Electrical Insulation. *IEEE Trans. Electr. Insul.,* Vol. EI-12, No. 1, (February 1977), pp. 2-18, ISSN 0018-9367.

Essam, J. W. (1980). Percolation theory. *Rep. Prog. Phys.,* Vol. 43, No. 7, (July 1980), pp. 53-134, ISSN 0034-4885.

Fothergill, J. C. (1990). Estimating the Cumulative Probability of Failure Data Points to be Plotted on Weibull and other Probalility Paper. *IEEE Trans. Electr. Insul.,* Vol. 25, No. 3, (June 1990), pp. 489-492, ISSN 0018-9367.

Fothergill, J. C. (1991). Filamentary Electromechanical Breakdown. *IEEE Trans. Electr. Insul.,* Vol. 26, No. 6, (December 1991), pp. 1124-1130, ISSN 0018-9367.

Fothergill, J. C. (1992). Filamentary Electromechanical Breakdown in Polymers. *Proceedings of the 4th International Conference on Conduction and Breakdown in Solid Dielectrics,* pp. 323-327, ISSN 0-7803-0129-3, Sestri Levante, Italy, June 22-25, 1992.

Frohlich, H. (1939). Dielectric Breakdown in Ionic Crystlas. *Phys. Rev.,* Vol. 56, No. 4, (August 1939), pp. 394-352, ISSN 0031-899X.

Hap, S. H. & Raju, G. G. (2006). DC Breakdown Characteristics of High Temperature Polymer Films. *IEEE Trans. Dielectr. Electr. Insul.,* Vol. 13, No. 4, (August 2006), pp. 917-926, ISSN 1070-9878.

Helgee, B. & Bjellheim, P. (1991). Electric Breakdown Strength of Aromatic Polymers: Dependence on Film Thickness and Chemical Structure. *IEEE Trans. Electr. Insul.,* Vol. 26, No. 4, (December 1991), pp. 1147-1152, ISSN 0018-9367.

Hikita, M.; Kanno, I; Ieda, M.; Ishino, I.; Doi, S. & Sawa, G. (1987). Electrical Breakdown of Ethylene Copolymers. *IEEE Trans. Electr. Insul.,* Vol. EI-22, No. 4, (April 1987), pp. 175-179, ISSN 0018-9367.

Hippel, A. V. & Alger, R. S. (1949). Breakdown of Ionic Crystals by Electron Avalanches. *Phys. Rev.,* Vol. 76, No. 1, (July 1949),pp. 127-133, ISSN 0031-899X.

Ieda, M. (1980). Dielectric Breakdown Processof Polymer. *IEEE Trans. Electr. Insul.,* Vol. EI-15, No. 3, (June 1980), pp. 206-217, ISSN 0018-9367.

Ieda, M. (1984). Electrical Conduction and Carrier Traps in Polymeric Materials. *IEEE Trans. Electr. Insul.,* Vol. EI-19, No. 3, (June 1984), pp. 162-179, ISSN 0018-9367.

Ieda, M. (1987). Carrier Injection, Space Charge and Electrical Breakdown in Insulating Polymers. *IEEE Trans. Electr. Insul.,* Vol. EI-22, No. 3, (June 1984), pp. 261-267, ISSN 0018-9367.

Job, A E; Alves, N.; Zanin, M.; Ueki, M. M.; Mattoso, L. H.; Teruya, M. Y. & Giacometti, J. A. (2003). Increasing the Dielectric Breakdown Strength of Poly (ethylene terephthalate) Films Using a Coated Polyaniline Layer. *J. Phys. D: Appl. Phys.,* Vol. 36, No. 12, (June 2003), pp. 1414-1418, ISSN 0022-3727.

Kim H K, Shi F G (2001). Thickness Dependent Dielectric Strength of a Low-permittivity Dielectric Film. *IEEE Trans. Dielectr. Electr. Insul.,* Vol. 8, No. 2, (June 2001), pp. 248-253, ISSN 1070-9878.

Laghari, J. R. & Sarjeant, W. J. (1992). Energy Storage Pulsed Power Capacitor Technology. *IEEE Trans. Power Electr.,* Vol. 7, No. 1, (June 2001), pp. 251-257, ISSN 0885-8993.

Laihonen, S. J.; Gafvert, U.; Schutte, T. & Gedde, U. W. (2007a). DC Breakdown Strength of Polypropylene Films: Area Dependence and Statistical Behavior. *IEEE Trans. Dielectr. Electr. Insul.,* Vol. 14, No. 2, (April 2007), pp. 275-286, ISSN 1070-9878.

Laihonen, S. J.; Gustafsson, A.; Schutte, T. & Gedde, U. W. (2007b). Area Dependence of Breakdown Strength of Polymer Films: Automatic Measurement Method. *IEEE Trans. Dielectr. Electr. Insul.,* Vol. 14, No. 2, (April 2007), pp. 263-274, ISSN 1070-9878.

Naidu, M. S. & Kamaraju, V. (1995). *High Voltage Engineering* (Second ed). McGraw-Hill Companies, Inc., ISBN 0-07-462286-2, New York, USA.

O'Dwyer, J. J. (1964). *Theory of Dielectric Breakdown in Solids*. Clarendon Press., ISBN 101-209-528 Oxford, U.K.

O'Dwyer, J. J. (1973). *The Theory of Electrical Conduction and Breakdown in Solid Dielectrics*. Calrendon Press., ISBN 0198513321, Oxford, U.K.

Pai, S. T., Zhang, Q. (1995). *Introduction to High Power Pulse Technology*. World Scientific Publishing Co. Pte. Ltd., ISBN 978-981-02-1714-3, Singapore.

Peruani, F.; Solovey, G.; Irurzun, I. M.; Mola, E. E.; Marzocca, A. & Vicente, J. L. (2003). Dielectric Breakdown Model for Composite Materials. *Phys. Rev. E,* Vol. 67, No. 6, (June 2003), pp. 1-6, ISSN 1550-2376.

Sarker, A. K.; Kimura, K; Yokoyama, F. & Yamashita, Y. (2001). Control of the Length of Aromatic Polyester Whiskers. *High Perform. Polym.,* Vol. 13, No. 2, (June 2001), pp. S351-S364, ISSN 0954-0083.

Sawa, G. (1986). Dielectric Breakdown in Solid Dielectrics. *IEEE Trans. Electr. Insul.,* Vol. EI-21, No. 6, (December 1986), pp. 841-846, ISSN 0018-9367.

Seeger, J. & Teller, E. (1939). Remarks on the Dielectric Breakdown. *Phys. Rev.,* Vol. 56, No. 4, (August 1939), pp. 352-354, ISSN 0031-899X.

Seitz, F. (1948). On the Mobility of Electrons in Pure Non-polar Insulators. *Phys. Rev.,* Vol. 73, No. 6, (March 1939), pp. 549-564, ISSN 0031-899X.

Stark, K. H. & Garton, C. G. (1955). Electric Strength of Irradiated Polythene. *Nature,* Vol. 176, (December 1955), pp. 1225-1226, ISSN 0028-0836.

Wang Z. D.; Chen, Z. T. & Wu, B. C. (1992). *Electrical Insulation Handbook*. (Second ed), China Machine Press, ISBN 7-111-00712-3, Beijing.

Wang, H. Y.; Ma, L. Y. & Zeng, Z. Z. (2004). Trigger Characteristics of Polymer-foil Switch with 1ns Delay and Sub-ns Jitter. *High Power Laser and Particle Beams,* Vol. 16, No. 12, (December 2004), pp. 1626-1628, ISSN 1001-4322.

Wang, H. Y.; Ma, L. Y. & Zeng, Z. Z. (2006). Sub-ns Jitter, 1ns Risetime and 10kV Rectangular Pulse Trigger Generator. *Plasma Science and Technology,* Vol. 8, No. 5, (September 2006), pp. 600-601, ISSN 1009-0630.

Wang, H. Y.; Ma, L. Y. & Zeng, Z. Z. (2008). Electric Breakdown Model for Dielectric Strength of 10μm Level Polyester Foil. *High Power Laser and Particle Beams,* Vol. 20, No. 10, (October 2008), pp. 1749-1752, ISSN 1001-4322.

Weibull, W. (1951). A Statistical Distribution Function of Wide Applicability. *J. Appl. Mechanics,* Vol. 9, (September 1951), pp. 293-297, ISSN 1528-9036.

Whitehead, S. (1951). *Dielectric Breakdown of Solids*. Oxford University Press., London and New York, 1951.

Wu, E. Y. & Vollertsen, R. P. (2002). On theWeibull Shape Factor of IntrinsicBreakdown of Dielectric Films and Its Accurate Experimental Determination —PartI: Theory, Methodology, Experimental Techniques. *IEEE Trans. Electron Devices,* Vol. 49, No. 12, (December 2002), pp. 2131-2140, ISSN 0018-9383.

Zakrevski, V. A.; Sudar, N. T.; Zappo, A. & Dubitsky, Y. A. (2003). Mechanism of Electrical Degradation and Breakdown of Insulating Polymers. *J. Appl. Phys.,* Vol. 93, No. 4, (February 2003), pp. 2135-2139, ISSN 0021-8979.

Zeller, H. R. & Schneider, W. R. (1984). Electrofracture Mechanics of Dielectric Aging. *J. Appl. Phys.,* Vol. 56, No. 2, (July 1984), pp. 455-159, ISSN 0021-8979.

Zeller, H. R.; Hibma, T. & Pfluger, P. (1984). Electrofracture Mechanics of Dielectric Aging. pp. 85-88, *1984 Annual Report Conf. Electr. Insul. and Dielectric Phenom*, ISSN 0084-9162, National Research Council (U.S.), Claymont, DE, October 21-25, 1984.